
Micro-Cooler for Chip-Level Temperature Control

Jeffrey Kirshberg and Dorian Liepmann
University of California at Berkeley

Kirk L. Yerkes
Air Force Research Laboratory AFRL/PRPG

SAE routinely stocks printed papers for a period of three years following date of publication. Direct your orders to SAE Customer Sales and Satisfaction Department.

Quantity reprint rates can be obtained from the Customer Sales and Satisfaction Department.

To request permission to reprint a technical paper or permission to use copyrighted SAE publications in other works, contact the SAE Publications Group.



GLOBAL MOBILITY DATABASE

All SAE papers, standards, and selected books are abstracted and indexed in the Global Mobility Database

ISSN 0148-7191

Positions and opinions advanced in this paper are those of the author(s) and not necessarily those of SAE. The author is solely responsible for the content of the paper. A process is available by which discussions will be printed with the paper if it is published in SAE Transactions. For permission to publish this paper in full or in part, contact the SAE Publications Group.

Persons wishing to submit papers to be considered for presentation or publication through SAE should send the manuscript or a 300 word abstract of a proposed manuscript to: Secretary, Engineering Meetings Board, SAE.

Printed in USA

Micro-Cooler for Chip-Level Temperature Control

Jeffrey Kirshberg and Dorian Liepmann
University of California at Berkeley

Kirk L. Yerkes
Air Force Research Laboratory AFRL/PRPG

ABSTRACT

The objective of this paper is to design and fabricate a micro-cooler to provide integral cooling to electronics or Microelectromechanical Systems (MEMS) type components utilizing current MEMS technologies. A three-port capillary pumped loop (CPL) was analyzed and fabricated from silicon and quartz for this purpose. An analytical study of the device is presented in support of this design. This proves the feasibility of such a device, and thus the rationale for continuing its development.

INTRODUCTION

In general there are many challenges in transitioning MEMS technologies to specific applications such as a micro-cooler that will benefit in cost, weight, manufacturing, reliability, etc. Specific technical challenges to the development of a micro-cooler include; (a) identification of potential micro-cooler thermodynamic processes, components, and geometries, (b) addressing the physics of micro scale heat transfer in solids, vapor, and liquids specific to micro-cooler geometries, (c) addressing the physics of phase change phenomena in the micro scale regime, (d) the development of macro scale to micro scale scaling laws specific to micro-cooler fluid systems, (e) addressing system level benefits as well as interfacing between the micro- to the macro-world, (f) modification of current or the development of new fabrication processes to allow the micro-cooler to be charged with the appropriate working fluid during fabrication, and (g) the development of appropriate calibration and testing diagnostics to verify micro-cooler performance.

There are numerous potential configurations for consideration when developing a micro-cooler. The micro-cooler may make use of micro scale phase change or single phase heat transfer to reject heat from electronics packages. Regardless of configuration, the micro-cooler will have to be able to fully control the movement of fluids through the system. The combination of micro scale heat transfer and fluid dynamics along with high surface to vol-

ume ratios will make the development of an efficient micro-cooler a challenging endeavor. Major components of the system may consist of a new family of pumps and valves to control liquid or vapor transport within the micro-cooler as well as innovative micro scale heat acquisition and heat rejection regions. Fluid actuators are more difficult in MEMS devices than in macro-systems because the planar nature of fabrication processes makes it difficult to make moving parts. As an alternative, we propose to utilize thermal actuation using bubbles to create both pumps and valves. This approach eliminates the need for moving parts and, perhaps more significantly, provides a system in which component failure, caused when a heating element burns out, can be easily sensed because the resistance becomes infinite. It is possible to design and fabricate back-up elements or use parallel circuits. Micro scale heat acquisition and heat rejection regions will incorporate micro-mixers potentially using enhanced surfaces to promote heat transfer, condensation, and boiling.

The objective of this paper is to present fundamental research efforts to making use of and evolving current MEMS technologies for the purpose of developing a micro-CPL to provide integral cooling to electronic or MEMS type components and systems. This paper will encompass the initial design of a three-port micro-CPL, schematically shown in Fig. 1, to be fabricated and assembled of micro-cooler components with final integration into a micro-cooler concept. It is important to realize that micro-devices can support extremely high gradients because of their small size. A mixer/evaporator configuration will be placed in direct contact with the micro-processor, sensor, or other electronic chip for which cooling is required and used to maintain an optimal temperature. The advantages of this approach are three-fold, first, precise temperature control at the chip-level, second, the overall cooling is more efficient because specific heat sources within the electronics package may be targeted, three, the overall size of the electronic system can be kept small.

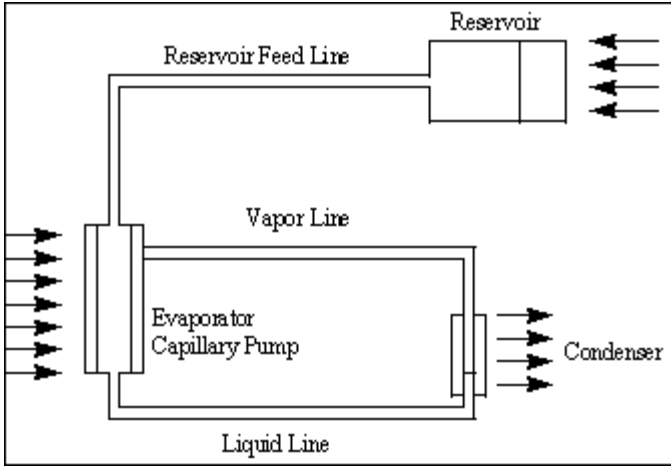


Figure 1. Schematic of a micro-CPL.

ANALYSIS

Table 1 provides specifications for two conceptual micro-CPLs with tubular or rectangular liquid/vapor line cross-sectional geometries. Both micro-CPL concepts consist of a planar evaporator and condenser with a grooved capillary wick structure..

Table 1. Micro-CPL specifications.

condenser area	2.5e+05 sq. micron	2.5e+05 sq. micron
evaporator length	1000 micron	1000 micron
groove height	50 micron	50 micron
groove width/number	50 micron/4	50 micron/4
vapor line	200 micron dia.	150x300 micron
liquid line	50 micron dia.	150x150 micron
max. Reynolds no.		
liquid line	Re= 16	Re= 28
vapor line	Re= 95	Re= 434

An analysis of the micro-CPL Capillary Pumping Limit was conducted following the rationale of Dickey and Peterson (1994) but including the pressure drop of the vapor line. This relationship was iteratively solved for the micro-CPL mass flow

$$\dot{m}^2 \left(\frac{c_p h_{fg}}{A_c h_c} \right) + \dot{m} \left[h_{fg} + c_p T_s - \left(\frac{c_p Q_T}{A_c h_c} \right) - c_p T_{w,c} \right] - Q_T = 0 \quad (1)$$

$$\bar{v} = \frac{\dot{m}}{rA} \quad (2)$$

while maintaining the following pressure relationship.

$$\Delta P_c + \Delta P_l + \Delta P_{bp} \geq \Delta P_w + \Delta P_l + \Delta P_v + \Delta P_g + \Delta P_f \quad (3)$$

Each pressure term in the above relationship represents a particular geometric portion of the micro-CPL for which the pressure balance must be maintained for proper CPL operation. Pressure terms ΔP_{bp} and ΔP_f represent micro-pump and micro-fence pressure drops which were not included in this analysis. The liquid and vapor lines were treated first as tubular transport lines, and then as

rectangular transport lines. The remainder of the pressure terms are assumed to have the following macro-scale relationships:

Capillary pressure drop,

$$\Delta P_c = \frac{2s}{r_c} = \frac{2s}{w} \quad (4)$$

Pressure drop due to the temperature gradient across the wick using the Clausius-Clapeyron equation,

$$\Delta P_t = \frac{h_{fg} P_v \Delta T}{RT_v^2} \quad (5)$$

Pressure drop across the wick structure,

$$\Delta P_w = \int_0^{L_e} \frac{m \dot{m}}{r_l A_w K} dx = \int_0^{L_e} \frac{m Q}{r_l h_{fg} A_w K} dx = \frac{m Q L_e}{r_l h_{fg} A_w K} = \frac{m Q L_e (f_l Re_l)(2h+w)^2}{8 r_l h_{fg} N_g (hw)^3} \quad (6)$$

Liquid line pressure drop in a circular tube,

$$\Delta P_l = r \left(\frac{64}{Re_l} \right) \left(\frac{L_l}{D_l} \right) \left(\frac{\bar{v}_l^2}{2} \right) \quad (7)$$

Liquid line pressure drop in a rectangular duct (Blevins, 1984),

$$\Delta P_l = r \left(\frac{64}{Re_l \left(\frac{2}{3} + 11/24 \left(\frac{h_l}{w_l} \right) \left(2 - \frac{h_l}{w_l} \right) \right)} \right) \left(\frac{L_l}{D_l} \right) \left(\frac{\bar{v}_l^2}{2} \right) \quad (8)$$

Vapor line pressure drop in a circular tube,

$$\Delta P_v = r \left(\frac{64}{Re_v} \right) \left(\frac{L_v}{D_v} \right) \left(\frac{\bar{v}_v^2}{2} \right) \quad (9)$$

Vapor line pressure drop in a rectangular duct (Blevins, 1984),

$$\Delta P_v = r \left(\frac{64}{Re_v \left(\frac{2}{3} + 11/24 \left(\frac{h_v}{w_v} \right) \left(2 - \frac{h_v}{w_v} \right) \right)} \right) \left(\frac{L_v}{D_v} \right) \left(\frac{\bar{v}_v^2}{2} \right) \quad (10)$$

The macro-scale auxiliary relationships of wick permeability,

$$K = \frac{2e r_{h,l}^2}{f_l Re_l} = \frac{8w(hw)^2 N_g}{f_l Re_l w_t (2h+w)^2} \quad (11)$$

Hydraulic radius,

$$r_{h,l} = \frac{2hw}{2h+w} \quad (12)$$

Wick porosity,

$$e = \frac{hwN_g L_e}{A_w L_e} = \frac{wN_g}{w_t} \quad (13)$$

And the friction relationship,

$$f_i Re_i = 24(1 - 1.3553a + 1.9467a^2 - 1.7012a^3 + 0.9564a^4 - 0.2537a^5) \quad (14)$$

were also used in this analytical approach.

RESULTS

Using water as a working fluid, assuming an operating temperature of 373 K and 3 degrees of subcooling with a condenser heat transfer coefficient of 10 W/sq. m-K, the maximum transport length for both cases is shown in Fig. 2. The results shown in Fig. 2 predict heat transport potential of 1.2e-02 W-m for the tubular transport lines, case a, and 8.0e-02 W-m for the rectangular transport lines, case b. By incorporating micro-pumping into the liquid line it may be possible to increase the heat transport potential thereby adding flexibility in applying the micro-CPL to specific cooling applications.

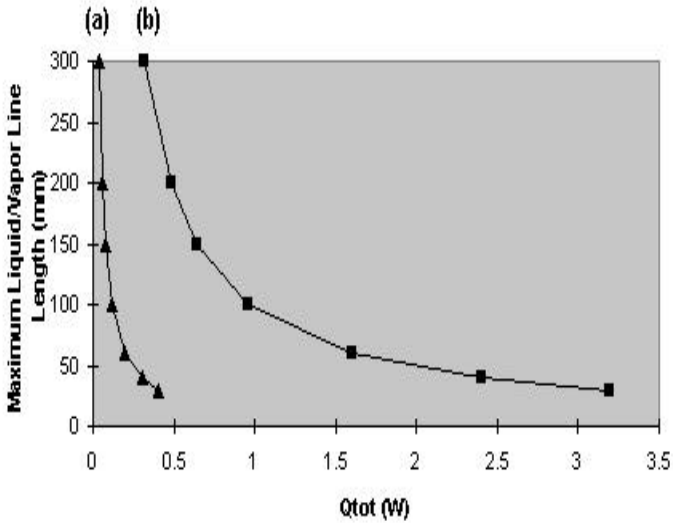


Figure 2. Maximum transport distance for; (a) cylindrical 200 micron vapor and 50micron liquid lines and, (b) rectangular 150x350 micron vapor and 150x150 micron liquid lines.

FABRICATION

Figure 3 illustrates the design of the micro-CPL. The evaporator, condenser, reservoir and liquid/vapor lines are fabricated from a single polished silicon wafer. The wicking structure consists of axial grooves wet etched into a standard quartz wafer, which serves as a coverplate. It is hypothesized that all evaporation will occur at the liquid/vapor interface in the wicking structure. How-

ever, in the event that bubbles form throughout the evaporator (which may well occur during start-up) posts were fabricated inside the evaporator to function as a fence prohibiting liquid from entering into the vapor line, which would cause device failure. A tube is connected to the back side of the silicon wafer via a through hole in order to function as the reservoir feed line.

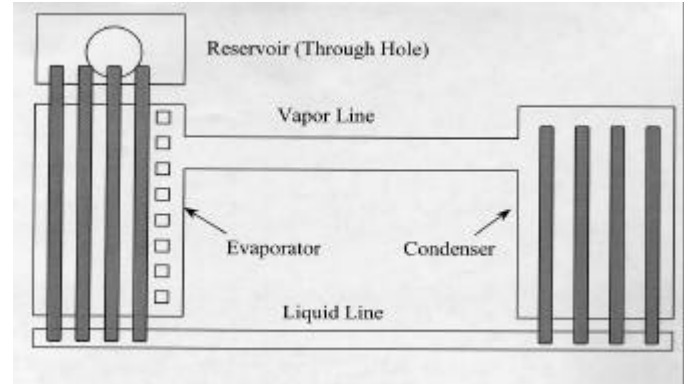


Figure 3. A sketch of the micro-CPL. The fluidic channels (white) are fabricated from silicon, while the wicking structure (gray) is etched into a quartz coverplate.

The fabrication of the fluidic channels in the silicon wafer requires two separate deep trench plasma etches. Initially, 2µm of Oxide were thermally deposited onto the wafer. A photoresist mask was then created on top of the oxide. The oxide was plasma etched in a Lam etcher in order to create an oxide mask for the wafer. 10µm of photoresist were then spun on top of the oxide mask, which once exposed, developed and baked, served as a mask for the through holes. A Surface Technology Systems deep trench plasma etcher was used to create the through holes. Once completed, the remaining photoresist was stripped thus revealing the oxide mask beneath it. The wafer was then deep trench etched 150µm, thus creating the fluidic channels. This process is outlined in figure 4.

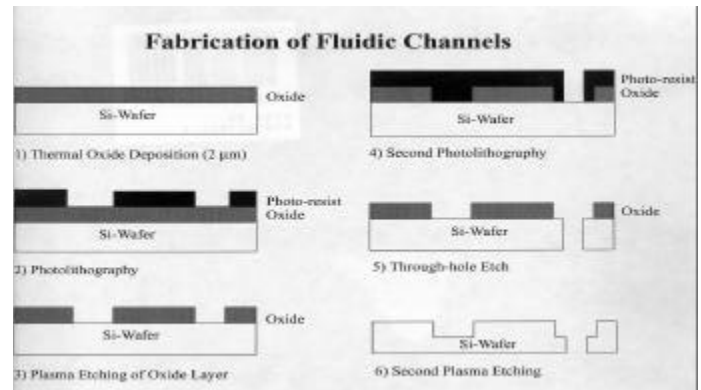


Figure 4. Fabrication process for the silicon wafer

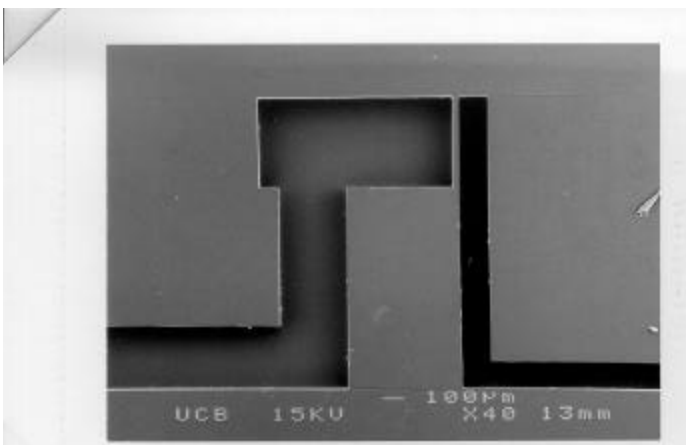
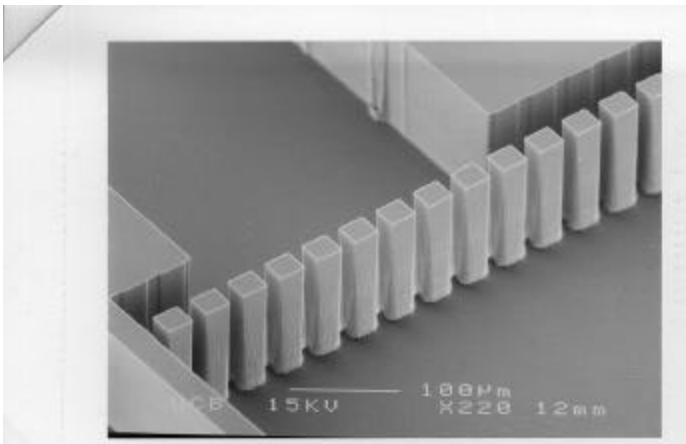
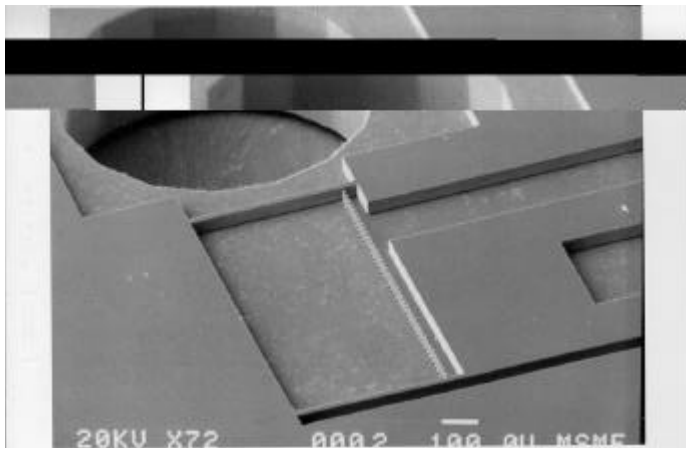


Figure 5. (a) A top view of the evaporator, reservoir, liquid and vapor lines. (b) $150\mu\text{m} \times 30\mu\text{m}$ posts in the evaporator region. (c) Top view of the condenser.

The wicking structure is fabricated in the Quartz coverplate. $1\mu\text{m}$ of undoped polysilicon was deposited on the quartz wafer. Quartz was chosen as opposed to glass due to the high temperatures required for this polysilicon deposition. A photoresist mask was then used when placing the wafer in silicon etchant. Once the silicon mask was complete, and the photoresist stripped, the device was placed in concentrated HF for 15 minutes. This isotropic etch created the hemispheric channels, with radius of $30\mu\text{m}$, which function as the wick in the micro-CPL. The process is outlined in figure 6.

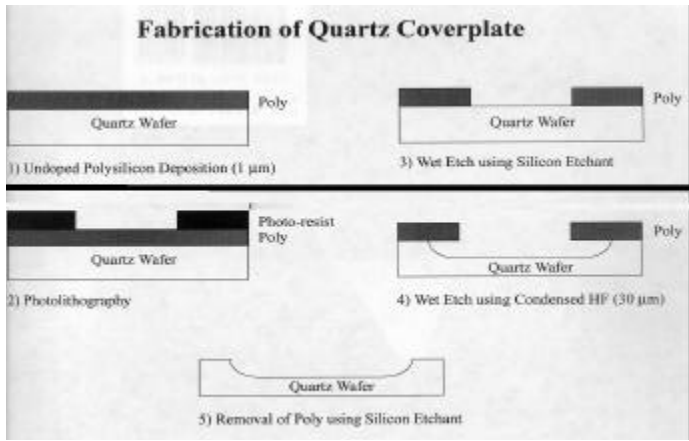


Figure 6. Fabrication process for the quartz wafer.

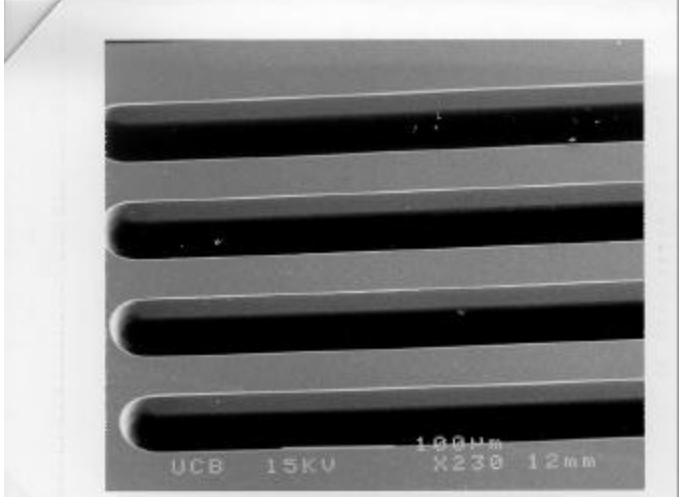
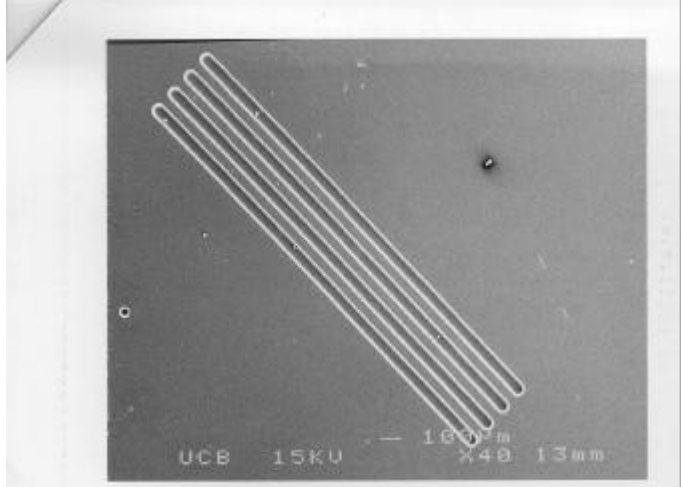


Figure 7. (a) A top view of the $1000\mu\text{m}$ long axial grooves wet etched into the quartz coverplate which function as the micro-CPL wicking structure. (b) The same axial grooves with radius $30\mu\text{m}$ at higher magnification.

Once these two wafers are cleaned, aligned and anodically bonded, the fabrication of the micro-CPL is complete.

CONCLUSION

With the design and fabrication of this micro-CPL completed, experimentation and optimization remain our final hurdles. By utilizing resistance heating and controlled spot cooling (e.g. a vortex tube), qualitative data can be gathered and analyzed using Digital Particle Image Velocimetry (DPIV). However, due to the small size scales of the micro-CPL, the insertion of a thermocouple into the liquid/vapor line must be approached cautiously, as such a device could seriously alter the physics of the micro-CPL.

Once the initial experimental results are obtained, there will be more insight into how to proceed with the development of a fully integrateable micro-CPL. Expected hurdles include the production of non-condensable gases in the evaporator and condenser regions, as well overcoming the startup transients inherent in a capillary pumped loop. It is only then that the three port micro-CPL can be fully utilized as a reliable cooling mechanism for electronic packages.

ACKNOWLEDGEMENTS

This research was sponsored by the Scientific and Technology Research Program for BMDO. The fabrication was done at the Berkeley Sensor and Actuator Center, and would not have been possible except for the constant advice and support of its members. A special thanks to Ron Wilson for all his help with the SEMS.

REFERENCES

1. Blevins, R.D., 1984, Applied Fluid Dynamics Handbook, Van Nostrand Reinhold Company, New York.
2. Cao, Y., Faghri, A., and Mahefkey, E.T., 1993, "Micro/Miniature Heat Pipes and Operating Limitations," Heat Pipes And Capillary Pumped Loops, The American Society of Mechanical Engineers.
3. Dickey, J.T. , and Peterson G.P. , 1994, "Experimental and Analytical Investigation of a Capillary Pumped Loop," *Journal of Thermophysics and Heat Transfer*, Vol 8, No. 3, pp. 602-607.
4. Faghri, A., 1995, Heat Pipe Science and Technology, Taylor & Francis, Washinton D.C.
5. Peterson, G.P., Duncan, A.B., and Weichold, M.H., 1993, "Experimental Investigation of Micro Heat Pipes Fabricated in Silicon Wafers," *Journal of Heat Transfer*, Vol 115, pp. 751-756.

NOMENCLATURE

A_c	= condenser surface area
A_w	= cross-sectional area of wick
c_p	= specific heat
D	= diameter

f	= friction factor
h	= groove height
h_c	= condenser convection coef.
h_{fg}	= latent heat of vaporization
K	= wick permeability
L	= length
\dot{m}	= mass flow rate
N_g	= groove number
P	= pressure
ΔP_c	= capillary pressure
ΔP_{bp}	= boost pressure due to micro-pump
ΔP_f	= vapor/liquid fence pressure losses
ΔP_g	= hydrostatic pressure losses
ΔP_l	= liquid pressure losses
ΔP_t	= pressure due to temp. difference
ΔP_v	= vapor pressure losses
ΔP_w	= pressure losses in wick
Q	= power
r_c	= capillary radius
r_h	= hydraulic radius
R	= gas constant
Re	= Reynolds number
T	= temperature
v	= velocity
w	= groove width
w_t	= total groove structure width
a	= groove aspect ratio
e	= wick porosity
m	= viscosity
ρ	= density
σ	= surface tension
<i>Subscripts</i>	
c	= condenser
e	= evaporator
l	= liquid
v	= vapor